

# Empty Helical Nanochannels with Adjustable Order from Low-Symmetry Macrocycles\*\*

Martin Fritzsche, Anne Bohle, Dmytro Dudenko, Ute Baumeister, Daniel Sebastiani, Gabriele Richardt, Hans Wolfgang Spiess, Michael Ryan Hansen,\* and Sigurd Höger\*

Natural channel-forming structures are mandatory for connecting different compartments within a living organism. For instance, transmembrane proteins function as ion channels, transporters, or antibiotics.<sup>[1]</sup> Biomacromolecules that are formed during evolution self-assemble into tubular structures with precisely defined positions of functional groups. The stimuli-responsive activity of these molecules has inspired the search for artificial channel-forming structures that can mimic the functionality of the natural systems.<sup>[2]</sup> Artificial channel systems may even include new functionalities in advanced chemical applications.<sup>[3]</sup> Several attempts, including templating methods,<sup>[4]</sup> have been reported for the de novo design of pore-forming structures that are stable both in solution and in the bulk state. In particular, macrocycles have an attractive topology for the formation of supramolecular channels if they organize in a columnar mesophase with close packing of successive rings.<sup>[5]</sup> If properly designed, a channel is created with tight walls that do not allow the penetration of small molecules. In contrast to macrocycles that are held together by strong intermolecular forces, such as hydrogen bonds in cyclopeptides<sup>[6]</sup> or cyclosaccharides,<sup>[7]</sup> the increased mobility in the liquid-crystalline (LC) phase allows for self-healing and orientation of the channels by external forces (shear, electro-

magnetic fields, surface properties, etc.).<sup>[8]</sup> When the channels are appropriately functionalized, the inclusion and manipulation of nano-objects becomes feasible.

Columnar mesophases have indeed been found in macrocyclic polyamines.<sup>[9]</sup> However, because of their flexibility, the macrocyclic rings assume a folded conformation and stable phases with large open voids have not been reported to date.<sup>[10]</sup> This problem might be overcome by using shape-persistent macrocycles,<sup>[11]</sup> and columnar liquid-crystalline compounds based on cyclic phenylene and phenylene-ethynylene oligomers with inner diameters of up to 1 nm, as deduced from X-ray diffraction studies (XRD), have been reported (Figure 1 a).<sup>[12]</sup> Powder XRD cannot provide details about the packing of the macrocycles on the molecular level,<sup>[4a,12c]</sup> whereas solid-state NMR spectroscopy can provide this information with the help of quantum-chemical calculations.<sup>[13]</sup> In contrast to diffraction techniques, NMR spectroscopy does not require strict periodicity and is therefore particularly suited to probe the local structure in LC phases. Moreover, NMR spectroscopy can be used to reveal the presence of guest molecules inside the channels, including back-folded side chains.<sup>[14]</sup>

Herein, we describe two phenylene-ethynylene-butydiynylene macrocycles **1a** and **1b** (Figure 1 b), each of which contains two benzo[1,2-b:4,3-b']dithiophene units that include a nanoscale interior with a diameter as large as approximately 1.3 nm (Figure 1 a). At the expense of symmetry, we have introduced groups with different electron affinities.<sup>[16]</sup> Both macrocycles **1a** and **1b** were obtained by the statistical oxidative Glaser coupling of the appropriate "half-rings" under Pd/Cu catalysis, and were obtained in yields of 33 % (**1a**) and 50 % (**1b**) after purification by recycling gel-permeation chromatography (recGPC) using THF as eluent, and subsequent precipitation from methanol and drying under vacuum. The compounds were obtained as slightly yellow powders that do not contain residual solvents as shown by NMR spectroscopy of solutions in dichloromethane (see the Supporting Information). Upon heating above room temperature, the compounds become waxy materials that are birefringent under optical microscopy (crossed polarizers). Differential scanning calorimetry (DSC) investigations (2nd heating; 10 °C min<sup>-1</sup>) showed reversible endothermic transitions for both compounds, thus indicating different LC phases over a broad temperature range (**1a**: 22 °C (138.9 kJ mol<sup>-1</sup>), 109 °C (85.2 kJ mol<sup>-1</sup>), 151 °C (2.8 kJ mol<sup>-1</sup>); **1b**: 33 °C (116.6 kJ mol<sup>-1</sup>), 160 °C (2.6 kJ mol<sup>-1</sup>)).

The type of LC phases formed and the lattice parameters were determined by XRD. Upon cooling from the isotropic

[\*] Dr. M. Fritzsche, Dr. G. Richardt, Prof. Dr. S. Höger  
Kekulé-Institut für Organische Chemie und Biochemie  
Rheinische Friedrich-Wilhelms-Universität Bonn  
Gerhard-Domagk-Str. 1, 53121 Bonn (Germany)  
Fax: (+49) 228-73 5662  
E-mail: hoeger@uni-bonn.de

Dr. A. Bohle, Dr. D. Dudenko, Prof. Dr. H. W. Spiess,  
Dr. M. R. Hansen  
Max-Planck-Institut für Polymerforschung  
Ackermannweg 10, 55128 Mainz (Germany)  
Fax: (+49) 6131-379 320  
E-mail: mrh@mpip-mainz.mpg.de

Dr. D. Dudenko, Dr. D. Sebastiani  
Fachbereich Physik  
Freie Universität Berlin  
Arnimallee 14, 14195 Berlin (Germany)

Dr. U. Baumeister  
Institut für Chemie, Martin-Luther-Universität Halle-Wittenberg  
Von-Danckelmann-Platz 4, 06120 Halle (Saale) (Germany)

[\*\*] We thank V. Enkelmann and G. Brunklaus for helpful discussions and P. Bednarek from the Informatikdienst der Universität Freiburg (Switzerland) for computational support. S. Pinnells is acknowledged for proofreading the manuscript. This work was financially supported by the DFG, the SFB 624 (Bonn) and SFB 625 (Mainz). D.S. acknowledges the DFG under grants Se 1008/5 and Se 1008/6.

Supporting information for this article is available on the WWW under <http://dx.doi.org/10.1002/anie.201007437>.

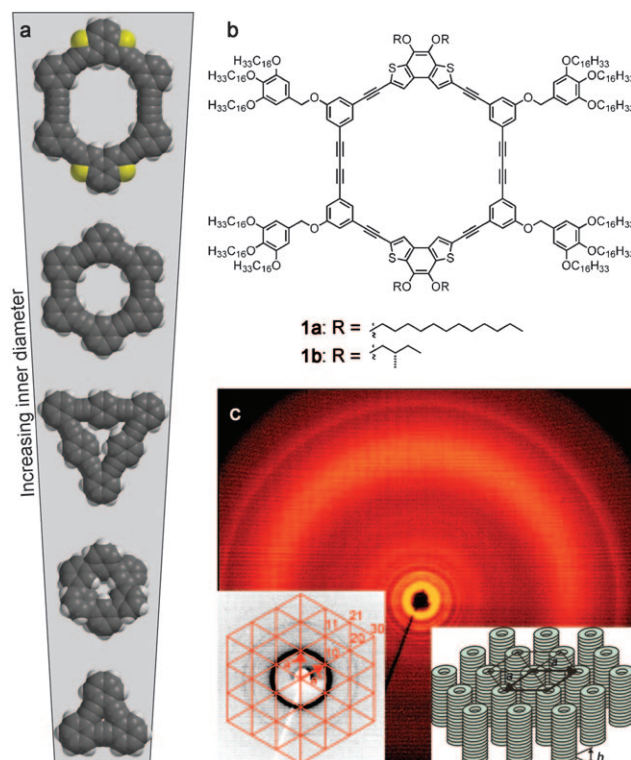


**Figure 1.** a) Relative size and symmetry of LC macrocycles<sup>[12a, c, 15]</sup> with inner diameters that range from 0.3 to 1.3 nm in our system. b) Chemical structures of compounds **1a** and **1b**. c) XRD pattern for a powderlike sample of **1a** at 60°C on cooling (lower part of the pattern shaded by the heating stage), left inset: small-angle region showing one orientation of the hexagonal reciprocal lattice with parameters  $a^*$  and the corresponding 2D indexing of the reflections; right inset: possible packing of the molecules in the hexagonal columnar structure showing the 2D hexagonal lattice with lattice parameters  $a = 5.31$  nm and the average stacking distance of the molecules within one column  $h = 0.35$  nm indicated by the outermost ringlike reflection in the wide-angle region.

melt, **1a** enters a high-temperature (HT) columnar LC phase with liquid-like order within the columns. The diffraction peaks in the small-angle area indicate a rectangular arrangement of the columns, that is, a  $\text{Col}_r$  phase (indexed according to a centered rectangular 2D unit cell,  $c2mm$ ;<sup>[17]</sup> see the Supporting Information). Upon further cooling, a low-temperature (LT) columnar phase with a hexagonal arrangement of the columns is observed (2D lattice parameters  $a = b$ ,  $\gamma = 120^\circ$ ;  $a = 5.31$  nm at 60°C; see Figure 1c and the Supporting Information). The outermost ringlike reflection at  $d \approx 0.35$  nm suggests  $\pi$ - $\pi$  stacking of the molecules along the columnar axes. The diffuse scattering in the wide-angle region ( $2\theta \approx 19^\circ$ ,  $d \approx 0.46$  nm) confirms the liquidlike disorder of the aliphatic chains in all mesophases. On the other hand, compound **1b** forms only a hexagonal phase with  $a = 5.13$  nm at 80°C (see the Supporting Information). Similar to the LT phase of **1a**, the correlation length of the molecular distances along the columnar axes increases with decreasing temperature, as indicated by the gradual sharpening of the outer part of the scattering curve at  $d \approx 0.35$  nm.

Both macrocycles adsorb onto highly-ordered pyrolytic graphite (HOPG) to form self-assembled monolayers

(SAMs), which were investigated by in situ scanning tunneling microscopy (STM). An STM image of **1a** at the HOPG/phenyloctane interface is shown in Figure 2b. Bright and dark colors indicate high and low local tunneling currents from

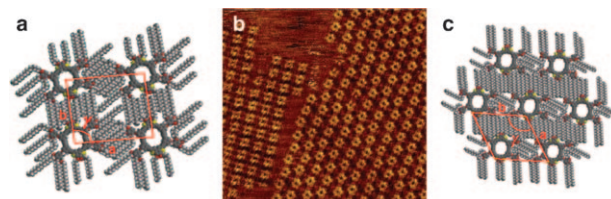


**Figure 2.** a, c) Molecular models for the SAMs of **1a** corresponding to oblique and pseudo-hexagonal lattices, respectively. b) STM image of **1a** at the phenyloctane/HOPG interface (image size:  $100 \times 100$  nm<sup>2</sup>,  $V_{\text{bias}} = -0.990$  V,  $I_t = 6$  pA).

unsaturated (rigid  $\pi$  system) and saturated (flexible alkyl fringe) segments. For both macrocycles, two different 2D structures coexist. For example, compound **1a** forms an oblique (nearly rectangular) pattern ( $a = (4.9 \pm 0.1)$  nm;  $b = (4.4 \pm 0.1)$  nm,  $\gamma = (94 \pm 1)^\circ$ ) as well as a pseudo-hexagonal pattern ( $a = (4.7 \pm 0.1)$  nm;  $b = (4.5 \pm 0.1)$  nm,  $\gamma = (121 \pm 1)^\circ$ ) in which adjacent molecules are linked by the interdigitating alkyl chains (Figure 2a, c). From the molecular dimensions and the lattice constants of the pattern in Figure 2b, which are consistent with the XRD data (Table S2), we conclude that the organization of the columns on the graphite surface in the LC phase is similar.<sup>[18]</sup>

Figure 3b shows the 2D NMR  $^{13}\text{C}\{^1\text{H}\}$  heteronuclear correlation (HETCOR) spectrum for compound **1a** in the LC phase. A remarkable spectral resolution is observed, with  $^{13}\text{C}$  linewidths in the order of approximately 100 Hz for the

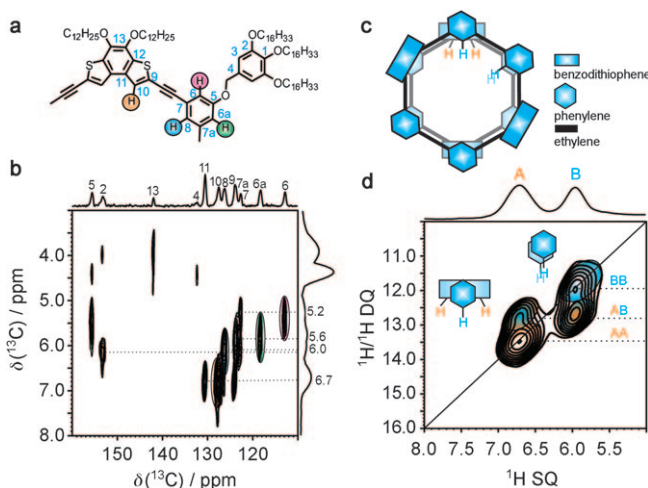


**Figure 3.** a) Assignment of the aromatic  $^{13}\text{C}$  and  $^1\text{H}$  resonances for **1a**. b) 2D  $^{13}\text{C}\{^1\text{H}\}$  FSLG-HETCOR spectrum of **1a** measured at 330 K, 15.0 kHz MAS, and a CP contact time of 3.0 ms. d) Fingerprint of the helical packing in **1a** from  $^1\text{H}$ - $^1\text{H}$  DQ-SQ correlation spectroscopy measured at 330 K, 25.0 kHz MAS, and one rotor period recoupling. The inset in (d) illustrates the observed intermolecular correlation peaks AB and BB, corresponding to a pitch angle of  $60^\circ$  between adjacent layers as schematically drawn in (c).

core of the macrocycle, thus implying a very high degree of local order.<sup>[19]</sup> The complete assignment given in Figure 3a is obtained from the 2D NMR spectrum in Figure 3b, and includes only one-quarter of the total number of  $^{13}\text{C}$  signals for the macrocycle, thus indicating that the macrocycles are located in highly symmetric environments, which can be envisaged in a helical arrangement of the macrocycles in a column. It should be noted that the ether bond through which the outer phenyl rings are attached to the macrocycle must be part of a constrained in-plane conformation of the  $\alpha\text{-CH}_2$  groups,<sup>[20]</sup> which makes the carbon atoms 6 and 6a inequivalent. A packing scenario that includes sliding of the macrocycles, such as the herringbone packing observed for hexa-*peri*-hexabenzocoronenes,<sup>[21]</sup> can be excluded, since this would lead to additional signals in the  $^{13}\text{C}$  NMR spectrum. The packing environment present in **1a** is also reflected in the  $^1\text{H}$  chemical shifts for the core protons of the macrocycle. These signals differ substantially from each other (Figure 3b), and also from the values found in solution (Table S5), which is a clear indication of  $\pi\text{-}\pi$  stacking.<sup>[22]</sup> The specific pitch angle can be determined by combining 2D NMR  $^1\text{H}\text{-}^1\text{H}$  DQ-SQ spectroscopy<sup>[13]</sup> with ab initio calculations. The strong auto-correlation peak BB observed in Figure 3d for the inner protons of the phenylene rings indicates that the two equivalent protons have a spatial proximity below 0.4 nm. This proximity can only result from an intermolecular contact as the intramolecular  $^1\text{H}\text{-}^1\text{H}$  distances for equivalent protons are around 0.7, 1.0, and 1.3 nm. Likewise, the cross-peak AB between the benzothiophene protons (A, orange) and the inner proton of the inner phenylene ring (B, blue) indicates a short inter-nuclear distance, which fixes the pitch angle between adjacent macrocycles to approximately  $60^\circ$  (inset in Figure 3d and Figure 3c). Within the stack, every fourth molecule is eclipsed, that is, related by translation, to result in a helical arrangement (Figure 4), as also observed in other self-assembled organic compounds.<sup>[8a,23]</sup>

The pitch angle of  $60^\circ$  is supported by the results from additional NMR experiments and ab initio calculations, which were carried out to investigate the packing of pairs of macrocycles by considering their energetics and the  $^1\text{H}$  chemical shifts of neighboring macrocycles (see the Supporting Information for details). Finally, ab initio calculations of  $^1\text{H}$  chemical shifts were performed for the complete helical channel structure as shown in Figure 4.<sup>[24]</sup> These calculations show excellent agreement between experimental and calculated values (Table S5).

Besides structural elucidation with atomic precision, NMR spectroscopy can also be used to investigate possible filling of the channels by solvent molecules, or the aliphatic side chains, which are invisible in diffraction experiments.<sup>[25]</sup> The  $^1\text{H}$  MAS NMR spectra (Figure S14) do not exhibit any sharp peaks, which would indicate mobile, trapped molecules, and the  $^{13}\text{C}\{^1\text{H}\}$  CP/MAS NMR spectra (Figures S15 and S16) do not reveal any signals that cannot be assigned other than to the macrocycle itself. This result is also consistent with NMR data of the compound in solution. Moreover, no indication of the proximity of the side chains to the macrocycles is observed, as would be revealed by  $\pi$  shifts or cross-peaks in 2D  $^1\text{H}\text{-}^1\text{H}$  DQ-SQ spectra (Figure S20). Thus, back-folding of

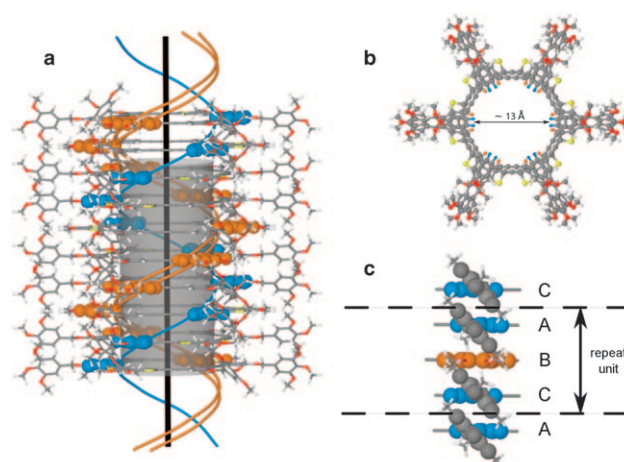


**Figure 4.** a) Helical stack with a pitch angle of  $60^\circ$ . b) Top view of the macrocycle (see STM results, Figure 3). c) Side-chain packing arrangement for illustrating the stabilizing effect of the outer phenylene groups. The blue and orange strings in (a) illustrate the helical pitch of the molecular stack. For clarity, side chains are represented as methoxy groups.

the side chains<sup>[14]</sup> can be excluded and the channels are clearly empty.

Replacement of the linear dodecyl chain on the condensed bithiophene by short branched 2-methyl-butyl side chains, as in **1b**, does not alter the overall supramolecular packing of the channels as deduced from XRD. This system, however, does not show the remarkable ordering of the macrocycle channels, as the resonances in  $^{13}\text{C}\{^1\text{H}\}$  CP/MAS NMR spectra **1b** in the LC phase are much broader (Figures S15 and S16). This observation suggests that the longer linear alkyl chains attached to the benzodithiophene units of the macrocycle play an important role in stabilizing the remarkably ordered intracolumnar packing of **1a** in the LC phase.

The helical stack shown in Figure 4a for **1a** is composed of a repeat unit of three molecules, which makes each fourth macrocycle identical and is consistent with the  $\text{C}_2$  symmetry of the macrocycle itself. The six inner aromatic moieties of one macrocycle have a total of 12 possible  $\pi\text{-}\pi$  contacts above and below the molecule. Eight of these contacts exploit the different electron affinities of phenylene and thiophene moieties ("donor-acceptor").<sup>[26]</sup> The outer dendritic phenyl rings stabilize the four repulsive contacts between like phenylene groups, which form pairs (two contacts per layer, in opposite directions) each with two of the in-plane alkoxy side chains and one out-of-plane side chain (Figure 4b,c). Such a delicate packing is difficult to envisage if the pitch angle in the helical stack is different from  $60^\circ$ , for example,  $0^\circ$  or  $30^\circ$ .

Although the macrocycles themselves only possess two-fold symmetry, it is surprising that they organize in columnar stacks in the LC phase with essentially sixfold symmetry. From a comparison of **1a** and **1b**, we conclude that the high order in **1a** results from a delicate interplay between the cores of the individual macrocycles (optimal  $\pi\text{-}\pi$  interactions) and the specific side chains attached to the benzodithiophene and inner phenylene groups. The short and branched chains of **1b**



appear to be less efficient in filling the space between the columns compared to those of **1a**. As a result, the local mobility of the macrocyclic core for **1b** is higher than that of **1a**, as deduced from additional solid-state NMR experiments. These experiments show that **1a** has a dynamical order parameter  $S \approx 1$ , whereas **1b** shows an increased mobility with  $S \approx 0.8$  (Figures S17 and S18).

The results presented here are based on a detailed structural investigation of shape-persistent macrocycles in the columnar LC phase by using complementary techniques. The shape-persistent rings in **1a** pack on top of each other without any spatial offset, thus leading to a tight tubular supramolecular superstructure. The side chains at the condensed bithiophene unit and the additional trialkoxybenzyl units at the ring periphery allow the formation of nano-channels by purely dissipative forces ( $\pi$ - $\pi$  interactions). Solid-state NMR spectroscopy unambiguously proves that the channels do not host solvent molecules or back-folded alkyl chains. Compound **1a** forms a particularly highly ordered columnar structure both in bulk and on graphite surfaces. Thus, even compounds with a reduced symmetry can organize in highly ordered columnar stacks with an almost perfect sixfold symmetry. This organization offers unforeseen freedom in the design of macrocycles to create highly functionalized alignable supramolecular nanochannels with uniform size. The internal order of the channels can be molecularly controlled and adjusted for future applications in recognition, stabilization, or organization of nanoparticles. Ongoing studies of symmetry-reduced macrocycles with different molecular structures are aimed at testing the selectivity of incorporation and verifying if tubes with an even larger inner diameter can be formed.

Received: November 26, 2010

Published online: February 15, 2011

**Keywords:** helical structures · liquid crystals · macrocycles · nanopores · solid-state NMR spectroscopy

- [1] M. Zasloff, *Nature* **2002**, *415*, 389–395.
- [2] a) J. M. Rausch, J. R. Marks, W. C. Wimley, *Proc. Natl. Acad. Sci. USA* **2005**, *102*, 10511–10515; b) M. A. B. Block, C. Kaiser, A. Khan, S. Hecht, *Top. Curr. Chem.* **2005**, *245*, 89–150.
- [3] a) T. Naddo, Y. Che, W. Zhang, K. Balakrishnan, X. Yang, M. Yen, J. Zhao, J. S. Moore, L. Zang, *J. Am. Chem. Soc.* **2007**, *129*, 6978–6979; b) Y. Baudry, G. Bollot, V. Gorteau, S. Litvinchuk, J. Mareda, M. Nishihara, D. Pasini, F. Perret, D. Ronan, N. Sakai, M. R. Shah, A. Som, N. Sorde, P. Talukdar, D. H. Tran, S. Matile, *Adv. Funct. Mater.* **2006**, *16*, 169–179.
- [4] a) G. Ferey, C. Mellot-Draznieks, C. Serre, F. Millange, J. Dutour, S. Surble, I. Margiolaki, *Science* **2005**, *309*, 2040–2042; b) V. Percec, A. E. Dulcey, V. S. K. Balagurusamy, Y. Miura, J. Smidrkal, M. Peterca, S. Nummelin, U. Edlund, S. D. Hudson, P. A. Heiney, D. A. Hu, S. N. Magonov, S. A. Vinogradov, *Nature* **2004**, *430*, 764–768; c) D. Y. Zhao, J. L. Feng, Q. S. Huo, N. Melosh, G. H. Fredrickson, B. F. Chmelka, G. D. Stucky, *Science* **1998**, *279*, 548–552.
- [5] D. Demus, J. Goodby, G. W. Gray, H. W. Spiess, V. Vill, *Handbook of Liquid Crystals*, Wiley-VCH, Weinheim, **1998**.
- [6] M. R. Ghadiri, J. R. Granja, R. A. Milligan, D. E. McRee, N. Khazanovich, *Nature* **1993**, *366*, 324–327.
- [7] P. R. Ashton, C. L. Brown, S. Menzer, S. A. Nepogodiev, J. F. Stoddart, D. J. Williams, *Chem. Eur. J.* **1996**, *2*, 580–591.
- [8] a) V. Percec, M. Glodde, T. K. Bera, Y. Miura, I. Shivanovskaya, K. D. Singer, V. S. K. Balagurusamy, P. A. Heiney, I. Schnell, A. Rapp, H. W. Spiess, S. D. Hudson, H. Duan, *Nature* **2002**, *419*, 384–387; b) L. Sardone, V. Palermo, E. Devaux, D. Credgington, M. De Loos, G. Marletta, F. Cacialli, J. Van Esch, P. Samori, *Adv. Mater.* **2006**, *18*, 1276–1280.
- [9] J. M. Lehn, J. Malthete, A. M. Levelut, *J. Chem. Soc. Chem. Commun.* **1985**, 1794–1796.
- [10] S. H. J. Idziak, N. C. Maliszewskij, P. A. Heiney, J. P. McCauley, P. A. Sprengeler, A. B. Smith, *J. Am. Chem. Soc.* **1991**, *113*, 7666–7672.
- [11] a) S. Höger, *J. Polym. Sci. Part A* **1999**, *37*, 2685–2698; b) W. Zhang, J. S. Moore, *Angew. Chem.* **2006**, *118*, 4524–4548; *Angew. Chem. Int. Ed.* **2006**, *45*, 4416–4439.
- [12] a) J. S. Zhang, J. S. Moore, *J. Am. Chem. Soc.* **1994**, *116*, 2655–2656; b) O. Y. Mindyuk, M. R. Stetzer, P. A. Heiney, J. C. Nelson, J. S. Moore, *Adv. Mater.* **1998**, *10*, 1363–1365; c) S. H. Seo, T. V. Jones, H. Seyler, J. O. Peters, T. H. Kim, J. Y. Chang, G. N. Tew, *J. Am. Chem. Soc.* **2006**, *128*, 9264–9265.
- [13] S. P. Brown, H. W. Spiess, *Chem. Rev.* **2001**, *101*, 4125–4155.
- [14] a) D. L. Morrison, S. Höger, *J. Chem. Soc. Chem. Commun.* **1996**, 2313–2314; b) S. Höger, V. Enkelmann, K. Bonrad, C. Tschierske, *Angew. Chem.* **2000**, *112*, 2355–2358; *Angew. Chem. Int. Ed.* **2000**, *39*, 2267–2270; c) M. Fischer, G. Lieser, A. Rapp, I. Schnell, W. Mamdouh, S. De Feyter, F. C. De Schryver, S. Höger, *J. Am. Chem. Soc.* **2004**, *126*, 214–222; d) S. Höger, X. H. Cheng, A. D. Ramminger, V. Enkelmann, A. Rapp, M. Mondeshki, I. Schnell, *Angew. Chem.* **2005**, *117*, 2862–2866; *Angew. Chem. Int. Ed.* **2005**, *44*, 2801–2805.
- [15] a) J. Luo, Q. Yan, Y. Zhou, T. Li, N. Zhu, C. Bai, Y. Cao, J. Wang, J. Pei, D. Zhao, *Chem. Commun.* **2010**, *46*, 5725–5727; b) W. Pisula, M. Kastler, C. Yang, V. Enkelmann, K. Müllen, *Chem. Asian J.* **2007**, *2*, 51–56.
- [16] T. Chen, G. Pan, H. Wettach, M. Fritzsche, S. Höger, L. Wan, H. Yang, B. H. Northrop, P. J. Stang, *J. Am. Chem. Soc.* **2010**, *132*, 1328–1333.
- [17] *c2mm* is the highest 2D symmetry compatible with the reflections only observed for Miller indices  $h + k = 2n$ , see *International Tables for Crystallography, Vol. A* (Ed.: T. Hahn), Kluwer Academic Publishers, Dordrecht, **1989**, p. 90, and one of the commonly found plane groups for the 2D lattices in columnar phases (corresponds to the planar space group *C2/m* assigned to these phases, see for example, Ref. [5], Vol. 2, Weinheim, Wiley, **1998**, chap. 8.
- [18] K. Praefcke, D. Singer in *Handbook of Liquid Crystals, Vol. 2B* (Eds.: D. Demus, J. W. Goodby, G. W. Gray, H. W. Spiess, V. Vill), Wiley-VCH, Weinheim, **1998**, pp. 945–967.
- [19] B. Elena, L. Emsley, *J. Am. Chem. Soc.* **2005**, *127*, 9140–9146.
- [20] J. Hirschinger, W. Kranig, H. W. Spiess, *Colloid Polym. Sci.* **1991**, *269*, 993–1002.
- [21] C. Ochsenfeld, S. P. Brown, I. Schnell, J. Gauss, H. W. Spiess, *J. Am. Chem. Soc.* **2001**, *123*, 2597–2606.
- [22] P. Lazzeretti, *Prog. Nucl. Magn. Reson. Spectrosc.* **2000**, *36*, 1–88.
- [23] a) F. J. M. Hoebe, P. Jonkheijm, E. W. Meijer, A. Schenning, *Chem. Rev.* **2005**, *105*, 1491–1546; b) X. Feng, V. Marcon, W. Pisula, M. R. Hansen, J. Kirkpatrick, F. Grozema, D. Andrienko, K. Kremer, K. Müllen, *Nat. Mater.* **2009**, *8*, 421–426.
- [24] D. Sebastiani, K. N. Kudin, *ACS Nano* **2008**, *2*, 661–668.
- [25] A. Hoffmann, D. Sebastiani, E. Sugiono, S. Yun, K. S. Kim, H. W. Spiess, I. Schnell, *Chem. Phys. Lett.* **2004**, *388*, 164–169.
- [26] C. A. Hunter, J. K. M. Sanders, *J. Am. Chem. Soc.* **1990**, *112*, 5525–5534.